Flexible simple-pole expansion of distribution functions

T. Löfgren* and H. Gunell
Division of Plasma Physics, Alfvén Laboratory, Royal Institute of Technology, SE-100 44 Stockholm, Sweden
(Dated: Recieved 4 March 1997; accepted 15 July 1997)

A method for parameterization and expansion of distribution functions is presented. The expansion has a finite number of simple poles, which gives efficient numerical calculations and control of all converging moments. The low velocity region is Maxwell-like and the high velocity tail follows an inverse power law. The method is applied to Maxwell-like distributions with and without suppressed tails. Dispersion relations can be obtained for a wide class of distributions, using building blocks available in any numerical library. Dispersion relations, for ordinary Langmuir waves and for beam-plasma interactions with intermediate temperature and beam to plasma density ratio, are derived. The Landau damping, obtained in the long wavelength regime, is of the same order but smaller than for the generalized Lorentzian distributions, for a given degree in the power law.

PACS numbers: 52.35.Fp 52.35.Qz 52.40.Mj

I. INTRODUCTION

In collisionless plasmas in space as well as in the laboratory, the electron distribution function $f(\mathbf{r},\mathbf{v})$ is often found to be non-Maxwellian. Loss cones and electrostatic sheaths (in e.g. a plasma diode) can cut the distribution for higher velocities. In natural space and astrophysical plasmas the distribution function often follows an inverse power law in the high energy tail $f \propto v^{-\alpha}$. There is a need for simple, flexible, distributions that more accurately describe those physical situations. It should be possible to increase or suppress the distribution in some velocity regions, and to cover plasmas in equilibrium states, the Maxwellian distribution should be a special case.

The description in this paper will be one dimensional, but the ideas are easily generalized to two or three dimensions. The Maxwellian distribution is numerically and theoretically problematic due to the essential singularity at infinity. The resonance distribution (or Lorentzian) $f_L \sim [1+v^2/(2v_t^2)]^{-1}$ gives simple calculations but it has large tails and infinite energy[1]. The multiplicity of the poles in the one-dimensional kappa-distribution (or generalized Lorentzian) $f_\kappa \sim [1+v^2/(2\kappa v_t^2)]^{-\kappa}$ introduces computational difficulties[2]. Using distribution functions with simple poles, the distribution function can be changed considerably without changing the numerical codes. It will be straight forward to include any characteristics from analog filters reducing or increasing desired part of the distribution.

This paper describes a method of expanding the Maxwellian distribution, that gives converging moments to any specified order with the tail following an inverse power law. All poles of this expansion are simple which gives short coded computations. Once the poles have been found it is cheap to calculate the converging moments and thus to normalize the distribution. A cut can be introduced in the tails by a mask that is multiplied with the ordinary expansion. Analog filters can be described by the complex poles and zeros of their transfer functions. Hence a mask can be introduced by including, in the distribution function, the poles and zeros of the transfer function of a suitable analog filter. A low-pass Butterworth filter has the desired properties, i.e., to suppress the high velocity parts without changing the distribution function for low velocities. It is a maximally flat approximation of the ideal low-pass filter. Its poles are equally spaced around the unit circle and its zeros are at infinity[3]. The final, normalized, expansion will be used to derive dispersion relations, for electrostatic linear waves in homogeneous Vlasov-plasmas, in one and multi component systems.

II. EXPANSION OF THE DISTRIBUTION FUNCTION

The plasma is assumed to be homogeneous and collisionless with an ion background of infinite mass. The electron distribution function f is Maxwell-like for moderate velocities but it is possible to introduce a cutoff at higher velocities. In a dimensionless (and not yet normalized) description, f can be written as a product

$$f(x) = M_w(x)T(x) \qquad x \equiv (v-v_d)/v_t \tag{1}$$

where M_w is a low-velocity (hence warm) expansion of the Maxwellian $f_0 = e^{\frac{-x^2}{2}}$ and T is a Butterworth mask with critical velocity x_0. v_d is the average drift and v_t is the standard deviation of the true Maxwellian. Note that this, v_t, is not the exact measure corresponding to the mean energy for distributions with truncated or thick tails. Taylor expanding $1/e^{\frac{x^2}{2}}$ the two factors read

$$\begin{cases} M_w(x) = \left[1+\frac{x^2}{2}+\ldots+\frac{1}{m!}(\frac{x^2}{2})^m\right]^{-1} \\ T(x) = \left[1+(\frac{x}{x_0})^{2n}\right]^{-1} \end{cases}. \tag{2}$$

The expansion M_w, displayed in Fig. 1a, is a generalization of the resonance distribution which corresponds to the special case $m=1$. The filter parameter n should be chosen to get the desired sharpness of the cutoff as

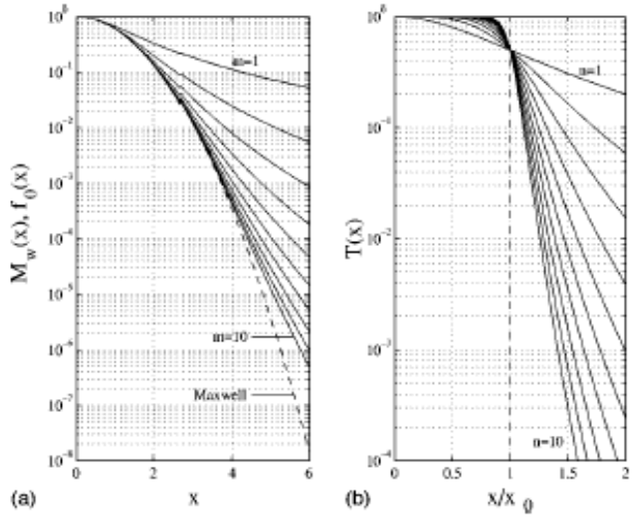

FIG. 1: (a) The Maxwellian f_0 (dashed) and the expansions M_w for $m = 1, \ldots, 10$ (solid). (b) The Butterworth mask for $n = 1, \ldots, 10$.

shown in Fig. 1b. Totally $m + n$ must be chosen high enough to get convergence of the desired moments and to suppress the distribution to required velocity, depending on the application. This sum could also be chosen to match an inverse power law since $f \propto x^{-(2m+2n)}$ as $x \to \infty$. If the distribution is chosen to approximate the Maxwellian distribution f_0, i.e., without cutoff ($n = 0$), it is necessary to check the validity of the Taylor expansion. The neglected terms in the full expansion are small (compared to 1) and fast decaying if $m! > (\frac{x^2}{2})^m$. Using the asymptotic behavior of the gamma function the condition becomes $|x|_{max} \sim \sqrt{m}$ for large m. The radius of convergence is thus asymptotically comparable to the kappa distribution which has $|x| \sim \sqrt{\kappa}$.[2] In the modeling of evanescent wave modes, the errors in the full complex plane are important. The error in the Taylor expansion, of f_0, in the complex plane is displayed in Fig. 2. The analytical continuation of f_0 is an entire function but M_w has poles in the finite complex plane. The absolute errors will however be small for all real x.

The poles of T which are analytically known ($x_0 e^{\frac{2p-1}{2n} i\pi}$, $p = 1, \ldots, 2n$), and of M_w found by standard numerical packages are in general simple. Factorization and decomposition of f into partial fractions result in an expression of the form

$$f = \sum_{i=1}^{2m+2n} \frac{a_i}{x - b_i}. \qquad (3)$$

When m, n are chosen, the residues a_i and poles b_i are calculated once and for all and f is normalized by dividing the residues with the zeroth moment. If the moment $\langle x^q \rangle = \int_{-\infty}^{\infty} f x^q dx$ does converge, it is possible to close the contour in the upper half plane, U, enclosing half of

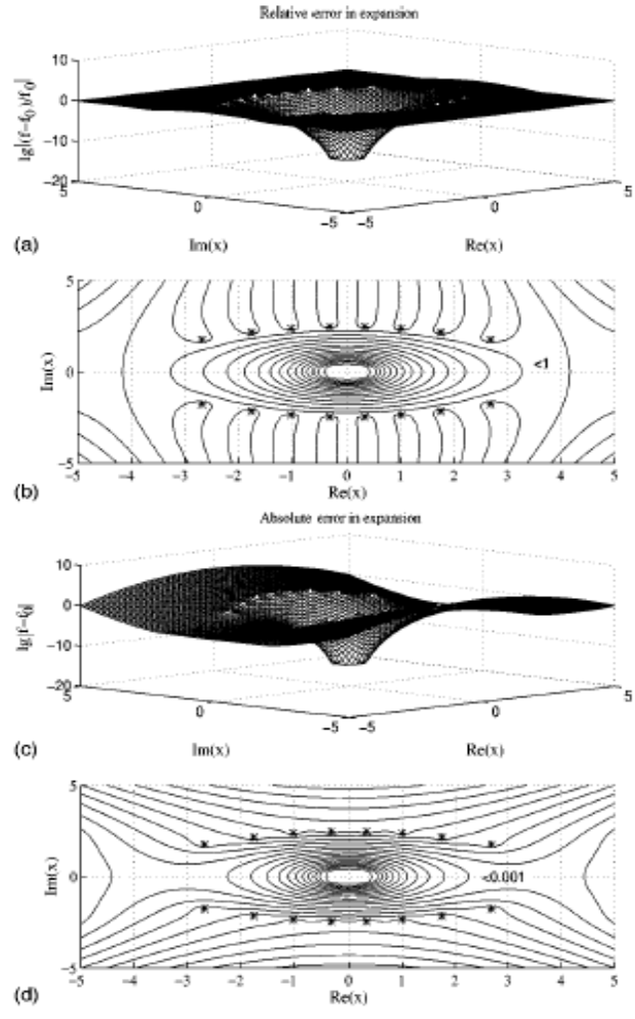

FIG. 2: The relative (a,b) and absolute errors (c,d) in the $m = 8$ expansion of $f_0 = e^{-\frac{x^2}{2}}$, with the poles b_i as stars. The contours are the powers of ten. The figures are based on a not normalized expansion. The lower limit of the errors are due to finite numerical resolution in the computations.

the poles, and get

$$\langle x^q \rangle = 2\pi i \sum_{b_i \in U} a_i b_i^q \qquad q < 2m + 2n - 1. \qquad (4)$$

The moments $\langle x^q \rangle$ of the normalized Maxwellian expansions ($n = 0, m$) are compared with the known even Maxwellian moments, given by $(q-1)!!$, in Table I. The average energy is well described by v_t using only a few terms. With $2m$ slightly higher than the highest required moment the "blow-up" of the highest moments is avoided. With the normalization of the expansion additional deviations from the Maxwellian distribution are introduced, see Fig. 3. The tails of M_w are broader than for the Maxwellian distribution which gives a reduction of the distribution function for low velocities.

The simple pole expansions in Eq. 3 can formally be

TABLE I: Moments $\langle x^q \rangle$ of the normalized distribution. The moments are related to the known Maxwellian moments which are given by $(q-1)!!$. The table entries are $\langle x^q \rangle/(q-1)!!$.

	$2m$						
q	4	6	8	10	12	14	16
2	2.83	1.38	1.14	1.06	1.03	1.01	1.01
4		4.44	1.71	1.27	1.12	1.06	1.03
6			5.94	2.02	1.40	1.19	1.10
8				7.37	2.32	1.53	1.26
10					8.77	2.62	1.66
12						10.16	2.91
14							11.53

used as a parameterization in a wide class of applications. The specific numbers (a_i, b_i) need not to be used until the final numerical computations.

III. DISPERSION RELATIONS

The dispersion relation in a one-component system, which will serve as an example, only defines one time and one length scale from the plasma frequency ω_p and the thermal velocity v_t. There is thus perfect scaling as long as the rest frame of a one component system is considered. For programming purposes the dimensionless variables are preferably kept, but for clarity in the derivation of the dispersion relations below variables with correct dimensions are reintroduced. The new variables will be marked with a tilde. The normalized distribution function is $\tilde{f} = \sum \frac{\tilde{a}_i}{v-\tilde{b}_i}$ with

$$\begin{cases} \tilde{a}_i = a_i \left[2\pi i \sum_{b_i \in U} a_i\right]^{-1} \\ \tilde{b}_i = b_i v_t + v_d \end{cases} . \tag{5}$$

where the residues and poles come from Eq. 3. The corresponding normalized Maxwellian is $\tilde{f}_0 = \frac{1}{v_t\sqrt{2\pi}} e^{-\frac{v^2}{2v_t^2}}$.

Dispersion relations will be studied in a linear, homogeneous, Vlasov-Poisson picture. The first order perturbation is of the form $e^{i(\omega t - kz)}$ (i.e., $\Im(\omega) < 0$ for growing modes) and the phase velocity is, by the Landau prescription[4], assumed to be in the lower half plane when deriving the dispersion relation. Accordingly, the integration contour can be closed in the upper half plane without enclosing the phase velocity pole, resulting in

$$1 = \omega_p^2 \int_{-\infty}^{\infty} \frac{\tilde{f} dv}{(\omega - kv)^2} = \omega_p^2 2\pi i \sum_{\tilde{b}_i \in U} \frac{\tilde{a}_i}{(\omega - k\tilde{b}_i)^2}. \tag{6}$$

No solution exists at the poles $\omega - k\tilde{b}_i = 0$, for finite wavelength, and the dispersion relation can be written as a polynomial in $\frac{\omega}{k}$ for a given $k \neq 0$.

$$\prod_i \left(\frac{\omega}{k} - \tilde{b}_i\right)^2 - \frac{\omega_p^2}{k^2} 2\pi i \sum_i \tilde{a}_i \prod_{j \neq i} \left(\frac{\omega}{k} - \tilde{b}_j\right)^2 = 0 \tag{7}$$

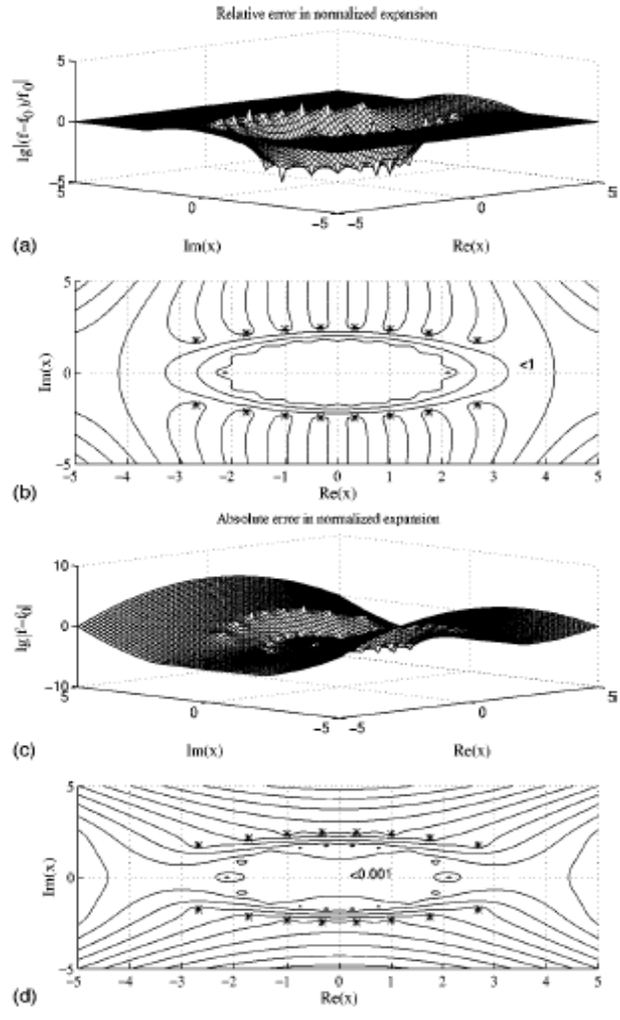

FIG. 3: The relative (a,b) and absolute errors (c,d) in the normalized $m = 8$ expansion of $f_0 = e^{-\frac{x^2}{2}}$, with the poles b_i as stars. The contours are the powers of ten. The expansion is normalized to $\sqrt{2\pi}$ (not 1) with the residue sum, $f = \sqrt{2\pi}\left[2\pi i \sum_{b_i \in U} a_i\right]^{-1} M_w(f_0)$, to make the absolute errors comparable with those in Fig. 2. The broader tails of M_w along the real axis give a reduction of the distribution function in the low-velocity region. The transit from overestimation to underestimation is seen as a wavy pattern in (b) and as islands in (d).

where the notation $\tilde{b}_i, \tilde{b}_j \in U$, i.e., restriction to the upper half plane, has been omitted in the summation and the products. Polynomial root finders in standard numerical packages can find the $2(m+n)$ roots. The roots are sorted to get $2(m+n)$ continuous wave modes $\frac{\omega}{k}(k)$, see Fig. 4.

In general $\tilde{f}$ can be used to model non-Maxwellian distributions. First the the errors introduced by using $\tilde{f}$, $(n = 0)$, approximating a true Maxwellian distribution, are discussed. There are two error types, denoted E1 and E2, introduced in the integration in Eq. 6. The open

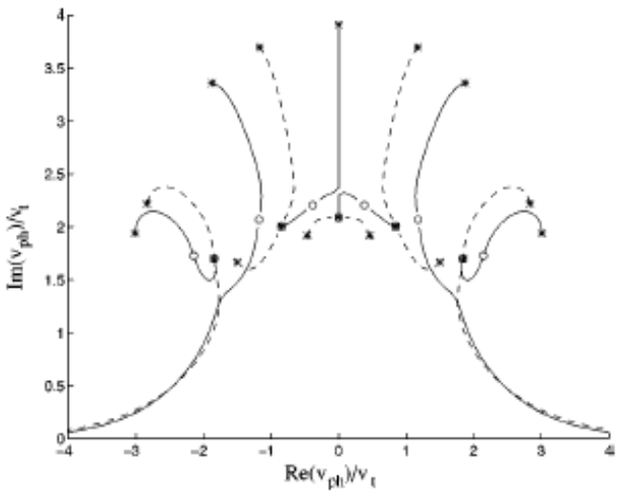

FIG. 4: Dispersion roots in complex phase velocity space with $k \in [2^{-5}, 2^4]\omega_p/v_t$ as parameter for the expansions $n = 0$ and $m = 6$ (solid) and $m = 5$ (dashed). The poles, $\tilde{b}_i$, are marked with circles and the limiting solutions $k \to 0$ ($v^0_{ph,r}$ in Eq. 15) are marked with stars. The Langmuir roots are only slightly modified, between the two expansions, for $\Im(\omega/k) < 1.3v_t$, but there is a large deviation close to the poles, where the waves are strongly damped. The correspondence between some $\tilde{b}_i$ and some $v^0_{ph,r}$ is a general property of the Maxwellian expansion, that disappears if the distribution is modified ($n > 0$). The authors have no explanation of this result. The poles will always be symmetric around the imaginary axis ($v_d = 0$), and purely imaginary poles are found for odd m.

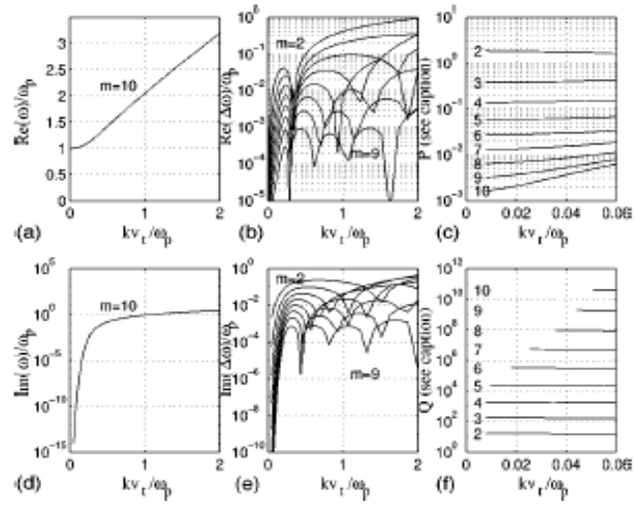

FIG. 5: The positive $\Re(\omega)$ Langmuir root for expansions $n = 0$ and $m \in [2, \ldots, 10]$. The upper panels (a-c) concern the real part and the lower panels (d-f) the imaginary part. The highest m solution is shown in (a,d). The difference in the solution $\Re(\omega(m) - \omega(m = 10))/\omega_p)$ and $\Im(\omega(m) - \omega(m = 10))/\omega_p$ is presented in (b,e) respectively. The real part is practically independent on m for $m > 4$. The absolute error in $\Im(\omega(m))$ is small but the relative error in the damping rate is large for low values of k. P in (c) is the function that makes $\omega = \omega_p\left(1 + \frac{3}{2}\omega_p^{-2}k^2v_t^2(1 + P(k))\right)$ an exact statement. If $P \ll 1$ the second moment is well described and if $k\partial P/\partial k \ll 1$, the curveform is quadratic. Q in (f) shows the behavior of the Landau damping, $Q = \frac{\Im(\omega)}{\omega_p}(\frac{kv_t}{\omega_p})^{-(2m-1)}$. The solutions in (d-f) with $\Im(\omega/\omega_p) < 10^{-14}$ have been omitted because of large numerical noise.

contour along the real axis with the phase velocity pole below the contour is considered.

(E1) Along the Cauchy principal integral at the real axis, an error is introduced in the averaging process. If the weight $\omega_p^2(\omega - kv)^{-2}$ is a slowly varying function for real v, it is sufficient to require small absolute errors in $\tilde{f}$ to avoid this error since the major contribution to the integral in Eq. 6 comes from the central part of the distribution. Then a small absolute error can be achieved with a few terms (m) for all phase velocities ($\Re(\omega/k)$) (Figs. 2 and 3). But if ω/k is close to the real axis the local error contribution must be small compared to the contributions to the integral near $v = 0$, i.e., $\left|\left[\tilde{f}(\Re(\frac{\omega}{k})) - \tilde{f}_0(\Re(\frac{\omega}{k}))\right]/\Im(\omega)^2\right| \ll \left|\tilde{f}(0)/\omega^2\right|$. The error is negligible if $\Re(\omega/k) < v_t\sqrt{2}(m!)^{1/2m}$.

(E2) The integration contour encircles the phase velocity pole (clockwise) if $\Im(\omega/k) > 0$. The residue $\frac{\partial \tilde{f}}{\partial v}(\omega/k)$ is well described in the same regions as $\tilde{f}$ in Figs. 2 and 3. Close to $\tilde{b}_i$, the expansion diverge and nonsensical results are expected. In contrast to E1, E2 only affects the upper half plane and the E2 error is most important if the damping is large.

Analytical solutions to Eq. 7 can be obtained in the two limits $k \to 0$ and $k \to \infty$. The Maxwellian approximation $n = 0, m \neq 0, v_d = 0$ will be examined as an example, but any normalized distribution that can be expressed as a simple pole expansion can be treated in the same way.

In the limit $k \to \infty$ the second term in Eq. 7 vanishes and a double root at each $\tilde{b}_i$ remains. By numbering the poles, different wave modes can be separated. The poles from M_w are artificial and a strong E2 error is introduced close to the poles. The poles from T are not artificial since they represent a physical cutoff in the distribution. With $\Im(\omega) = k\Im(\tilde{b}_i) \to \infty$, no solution in this regime is interesting, since they are strongly damped. By the numerical solution in Fig. 5, it is seen that the approximation is acceptable for all reasonable dampings (and $m > 4$). Note that all solutions (for all distributions) are damped for wavelengths short enough.

In the limit $k \to 0$, the roots $\omega = \mathcal{O}(1)$ are found by expanding the denominator in the sum of Eq. 6 in the

limit $k/\omega \to 0$

$$\omega^2 = \omega_p^2 2\pi i \sum_{\tilde{b}_i \in U} \left[\tilde{a}_i \sum_{j=0}^{\infty} (j+1) \left(\frac{k\tilde{b}_i}{\omega} \right)^j \right] = \omega_p^2 \sum_{j=0}^{2m-2} (j+1) \left(\frac{k}{\omega} \right)^j \langle v^j \rangle + \omega_p^2 2\pi i \sum_{\tilde{b}_i \in U} \left[\tilde{a}_i \sum_{j=2m-1}^{\infty} (j+1) \left(\frac{k\tilde{b}_i}{\omega} \right)^j \right] \quad (8)$$

where the last equality follows from the converging moments in Eq. 4. Note that since there is a finite number of converging moments, it is not possible to interchange the integration and the limit $k/\omega \to 0$ in Eq. 6. The two Langmuir roots, $\omega = \mathcal{O}(1)$, are found by using that $\tilde{f}$ is normalized ($2\pi i \sum \tilde{a} = 1$), i.e., $\omega = \pm\omega_p + \mathcal{O}(k)$. Let $\omega_q(k) = \omega_p + \delta_1 + \ldots + \delta_q$ be the solution to the order k^q. Keep terms to k^q in Eq. 8 and multiply with ω_q^q

$$(\omega_{q-1} + \delta_q)^{q+2} + \mathcal{O}(k^{q+1}) = \omega_p^2 2\pi i \sum_{\tilde{b}_i \in U} \left[\tilde{a}_i \sum_{j=0}^{q} (j+1)(k\tilde{b}_i)^j (\omega_{q-1} + \delta_q)^{q-j} \right] \quad (9)$$

The solution to $\mathcal{O}(k^q)$ is

$$(\omega_{q-1})^{q+2} + (q+2)\omega_p^{q+1}\delta_q + \mathcal{O}(k^{q+1}) = q\delta_q\omega_p^{q+1} + \omega_p^2 2\pi i \sum_{\tilde{b}_i \in U} \left[\tilde{a}_i \sum_{j=0}^{q} (j+1)(k\tilde{b}_i)^j (\omega_{q-1})^{q-j} \right] \quad (10)$$

where one of the $j = 0$ terms is moved out of the summations. This linear equation in δ_q gives

$$\delta_q = \tfrac{q+1}{2}\omega_p 2\pi i \sum_{\tilde{b}_i \in U} \tilde{a}_i \left(\frac{k\tilde{b}_i}{\omega_p} \right)^q + \mathcal{O}(k^{q+1}) + \tfrac{1}{2}\omega_p^{-q} \left[\omega_p^2 2\pi i \sum_{\tilde{b}_i \in U} \left[\tilde{a}_i \sum_{j=0}^{q-1} (j+1)(k\tilde{b}_i)^j (\omega_{q-1})^{q-1-j} \right] - (\omega_{q-1})^{q+1} \right] \quad (11)$$

The first term is the contribution from the extra k^q term in Eq. 8. The last terms seem to include lower order corrections, but by replacing q by $q-1$ in Eq. 9 it is clear that these terms are a first correction to the error made in the previous step, and thus $\mathcal{O}(k^q)$. The higher order terms should be removed out of this sum. To save some tedious bookkeeping this step is formally included in the additional term $\mathcal{O}(k^{q+1})$.

As a first example of Eq. 11, the resonance distribution ($m = 1$) gives $\delta_1 = 2\pi i a k b = i\sqrt{2}kv_t$, which in fact is the exact solution[1]. The second example is a distribution with converging energy ($m \geq 2$). The first order correction vanishes for a symmetric distribution and the second order correction $\delta_2 = \frac{3}{2}\omega_p^{-1}k^2\langle v^2 \rangle$ gives the Bohm-Gross dispersion relation $\omega_2 = \omega_p\left(1 + \frac{3}{2}\omega_p^{-2}k^2\langle v^2 \rangle\right)$. In this limit the real part gives the same result as for the Maxwellian distributions and as for the generalized Lorentzian[5]. The apparent deviation in the second moment in Table I only implies that the thermal velocity v_t, as defined in this paper, does not exactly represent the standard deviation of the distribution function $\tilde{f}$.

TABLE II: Normalization factor $N(m) = \sqrt{2\pi}[2\pi i \sum_{b_i \in U} a_i]^{-1}$.

m	1	2	3	4	5	6	7	∞
$N(m)$	$\pi^{-1/2}$	0.877	0.957	0.983	0.993	0.997	0.999	1

The terms $2\pi i \sum \tilde{a}_i \tilde{b}_i^q$ in Eq. 11 are in general complex numbers. But to all orders q of converging moments $\langle v^q \rangle = 2\pi i \sum \tilde{a}_i \tilde{b}_i^q \in \Re$ and thus the corrections δ_q are real. The Landau damping will come from the first non-converging moment, i.e., $\Im(\omega) \sim \mathcal{O}(k^{2m-1})$. In the limit $m \to \infty$, the damping is of infinite order which is well known for Maxwellian distributions, but for all finite m the damping is overestimated due to the broader tails. Both E1 and E2 errors contribute. The order of the damping rate is determined by the first non-converging moment in any simple-pole expansion. Closer estimates of the damping rate in the special case of the M_w distribution can be obtained from the asymptotic behaviour of M_w in the limit $v \to \infty$,

$$\tilde{f} = \frac{N(m)}{v_t\sqrt{2\pi}} 2^m m! \left[\frac{v}{v_t} \right]^{-2m}. \quad (12)$$

The normalization constant of order unity $N(m) = \sqrt{2\pi}[2\pi i \sum_{b_i \in U} a_i]^{-1}$, tabulated in Tab. II, is calculated by numerical methods presented in section II. The damping rate is found by integrating a half turn around the phase velocity pole using the asymptotic distribution function in Eq. 12

$$\Im(\omega) = -\omega_p \frac{\pi\omega_p^2}{2k^2} \left[\frac{\partial \tilde{f}}{\partial v} \right]_{\frac{\omega_p}{k}} = \omega_p m 2^m m! \sqrt{\frac{\pi}{2}} N(m) \left[\frac{kv_t}{\omega_p} \right]^{2m-1}. \quad (13)$$

The increased damping rate in the high phase velocity region has also been reported for the generalized Lorentzian distribution[6]. The generalized Lorentzian distribution has an asymptotic damping rate

$$\Im(\omega) = \omega_p \kappa 2^\kappa \kappa! \sqrt{\frac{\pi}{2}} \frac{\kappa^{\kappa-3/2}}{\Gamma(\kappa - \frac{1}{2})} \left[\frac{kv_t}{\omega_p} \right]^{2\kappa-1}. \quad (14)$$

with asymptotic distribution function $f_\kappa \sim v^{-2\kappa}$ where κ is the spectral index[5]. The M_w expansion thus has the same order of the Landau damping as the generalized Lorentzian distribution for given degree of the high velocity power law. The constant of proportionality differs considerably for higher m, κ. The factor of order unity $N(m)$ in Eq. 13 has been replaced by $\frac{\kappa^{\kappa-3/2}}{\Gamma(\kappa-\frac{1}{2})} \to \frac{e^\kappa}{\sqrt{2\pi\kappa}}$ as $\kappa \to \infty$ in Eq. 14. The kappa distribution thus gives higher damping rate than the M_w expansion for a given degree in the power law.

The Langmuir roots from numerically calculated dispersion relations are presented in Fig. 5 for different expansions m. The real part is almost independent of m

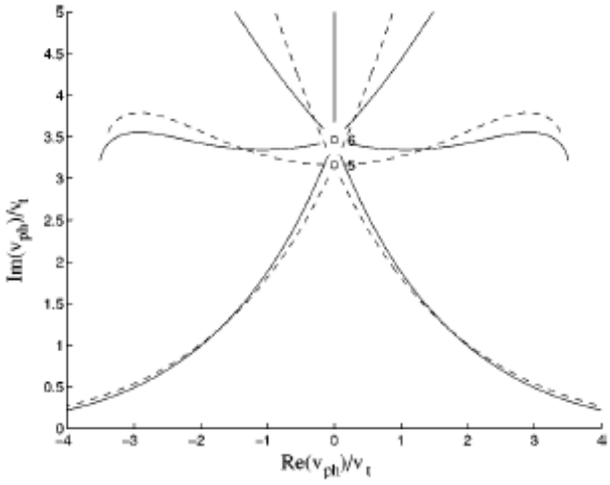

FIG. 6: Dispersion roots for the generalized Lorentzian distribution in complex phase velocity space with $k \in [2^{-5}, 2^{12}]\omega_p/v_t$ as parameter for the expansions $\kappa = 6$ (solid) and $\kappa = 5$ (dashed). The poles, $\sqrt{2\kappa}v_t i$, are marked with circles. There are $\kappa + 1$ solutions. The two Langmuir roots are only slightly modified, between the two expansions, for moderately damped waves. The other roots are strongly damped.

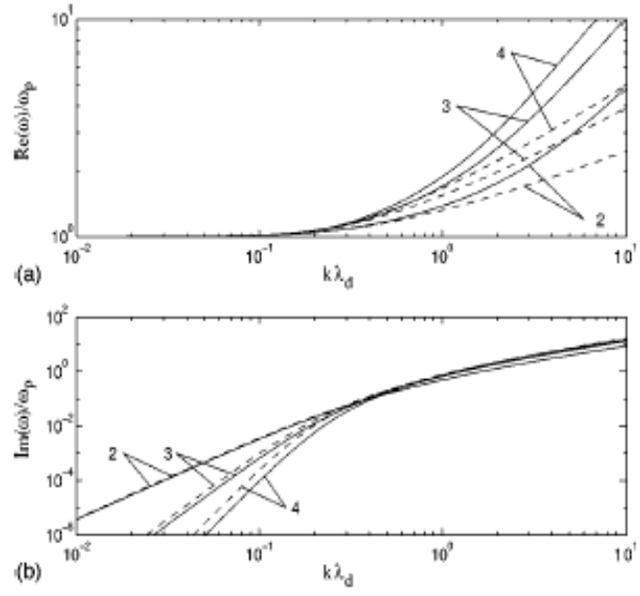

FIG. 7: The positive $\Re(\omega)$ Langmuir root for the M_w expansion (solid) and the generalized Lorentzian distribution (dashed) with $m, \kappa \in [2, 3, 4]$. The upper panel (a) concern the real part and the lower panel (b) the imaginary part.

when $\Im(\omega) < \omega_p$ and $m > 4$, but the relative error in $\Im(\omega)$ is important for low values of k. The behavior of the solutions in the low k limit, i.e., the quadratic real part and the damping rate of the order $\mathcal{O}(k^{2m-1})$, is numerically confirmed.

The remaining roots, in the limit $k \to 0$, are $\mathcal{O}(k)$ and they are found as zeros to the second term in Eq. 7, i.e., $\omega = kv^0_{ph,r} + \mathcal{O}(k^2)$, where $v^0_{ph,r}$ solves

$$\sum_i \tilde{a}_i \prod_{j \neq i} \left(v^0_{ph,r} - \tilde{b}_j \right)^2 = 0 \qquad (\tilde{b}_j \in U). \tag{15}$$

The zeros $v^0_{ph,r}$ will always be in the upper half plane for one component expansions of the type $M_w T$, since these are stable by the Penrose condition.

The presented expansions M_w are identical with the generalized Lorentzian distributions $f_\kappa \sim [1 + v^2/(2\kappa v_t^2)]^{-\kappa}$ for $m, \kappa = 1$ and in the limit $m, \kappa \to \infty$. It is of some interest to compare the dispersive characteristics in the intermediate range of m and κ. The plasma dispersion function for the kappa distribution is given in Summers and Thorne[2] Eq. 20, and the dispersion relation for electrostatic waves is found in Thorne and Summers[6] Eq. 3. The dispersion relation is a rational expression and the solutions can be found by standard numerical packages. The waves in complex phase velocity space are shown in Fig. 6 using the same Fourier representation of the modes as in this paper, i.e., damped solutions in the upper half plane. To compare the positive Langmuir root more in detail, the modes are presented in the same diagrams in Fig. 7. The thermal velocity v_t is not directly comparable between the two expansions. Therefore energy normalization is chosen by the use of the Debyelength λ_D. This is related to the velocity v_t by $\lambda_D =< x^2 >^{\frac{1}{2}} \frac{v_t}{\omega_p}$ and $\lambda_D = \sqrt{\frac{2\kappa}{2\kappa - 3}} \frac{v_t}{\omega_p}$ respectively. The kappa distribution predicts lower frequencies in the short wavelength regime. For $k \to 0$ the M_w expansion has lower damping rate but $\Re(\omega)$ converges between the two expansions.

IV. BEAM-PLASMA EXAMPLE

In a system which can be described by a collection of components (l), with different drifts $(v_{d,l})$, temperatures $(v_{t,l}, (x_{0,l}))$, densities $(\omega^2_{p,l})$ and expansions (m_l, n_l) the dispersion relation formally reads

$$1 = 2\pi i \sum_l \left[\omega^2_{p,l} \sum_{\tilde{b}_{i,l} \in U} \frac{\tilde{a}_{i,l}}{(\omega - k\tilde{b}_{i,l})^2} \right]. \tag{16}$$

where each component is normalized as $2\pi i \sum_i \tilde{a}_{i,l} = 1$. What is said in previous section is still valid since this also represents a simple pole expansion. All roots are strongly damped for short wavelengths, and the Langmuir roots still follow $\omega = \pm\omega_p + \mathcal{O}(k)$, where $\omega_p^2 = \sum_l \omega^2_{p,l}$. By performing the analysis for δ_q in analogy with the one component system, the solution becomes $\omega = \pm\omega_p + k \sum_l \frac{\omega^2_{p,l}}{\omega_p^2} v_{d,l} + \mathcal{O}(k^2)$, i.e., Langmuir waves Doppler shifted by the weighted mean velocity. If all components (l) represent particles with the same mass (e.g. electrons), this is is a centre of momentum Doppler

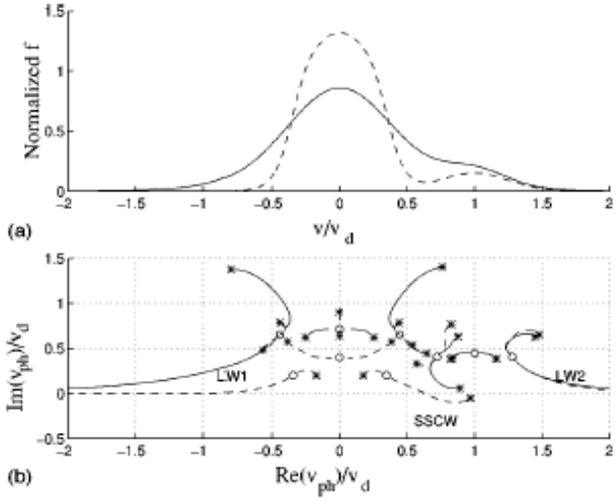

FIG. 8: (a) The normalized distribution functions for parameters in Table III, A1 (solid) and A2 (dashed). (b) Dispersion roots in complex phase velocity space with $k \in [2^{-5}, 2^4]\omega_p/v_d$ as parameter for the distributions in (a). The poles, $\tilde{b}_i$, are marked with circles and the limiting solutions $k \to 0$ ($v^0_{ph,r}$ in Eq. 15) are marked with stars. The poles are centred around the component drift velocities and the lowest lying poles only exist for the parameters according to A2 in table III.

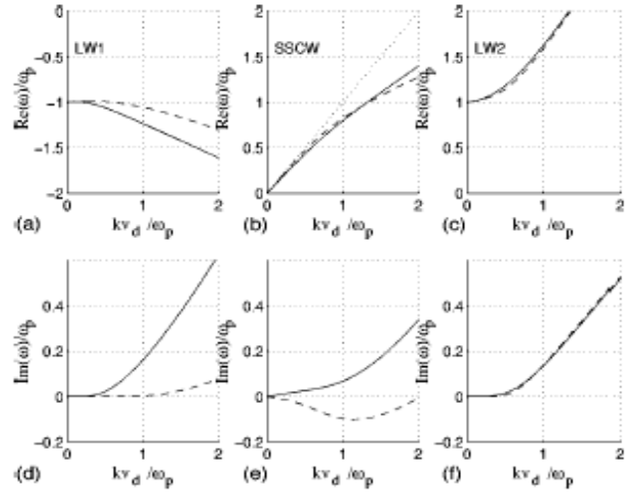

FIG. 9: The three most important dispersion roots for parameters in Table III, A1 (solid) and A2 (dashed). The first row (a-c) gives the real part and the second row (d-f) shows the corresponding imaginary part. A reference line $\omega = kv_d$ is introduced in (b)

shift. Some of the $\mathcal{O}(k)$ solutions may be growing in this multiple component system.

The beam-plasma interaction will be used to show the usefulness of this parameterization technique for non-Maxwellian distributions with strong beams and intermediate temperatures, i.e., regions not reachable by ordinary limit solutions. Those parameter regions are common at e.g. the high potential side in double-layer experiments and in some beam plasma experiments[7,8]. At a double layer the electron beam is accelerated in the potential well from the (warm) plasma. Since the double layer potential drop ϕ_{DL} can be of the same order as $\frac{k_B T_e}{e}$, the contraction of the distribution in the acceleration phase is small, and a much broader distribution is achieved than in electron gun or cathode experiments. In mirror field configurations or at the boundaries in a plasma diode, the high energy tail is lost. Two distributions with parameters in Table III will be examined. A stable distribution (A1) is turned unstable (A2) by an introduced cut in the tail. A low degree of the expansion parameters m, n is chosen to make the figures more readable.

The roots in complex phase velocity plane are shown in Fig. 8. The marked waves span different phase velocity regions and the roots will be named from the behaviour *in the long wavelength regime*. The Langmuir roots will never intersect the Doppler shifted beam roots, and the roots are strongly perturbed. It is straight forward to use this method to study topological shifts as presented in O'Neil and Malmberg[9]. The shift from "Dirac-delta beam" as in the presented result to "gentle bump" type solutions, i.e., when the forward Langmuir root (LW2) connects to a pole with $\Re(\tilde{b}_i) < v_d$, appears in strongly damped regions because of the broad distributions. For temperatures and expansions as in A1 (Table III) the mode shift is at $\omega^2_{p,2} \sim 0.0036\omega^2_p$. The forward Langmuir root (LW2) is only slightly modified by the cut in the distribution, but the backward root (LW1) has a strongly reduced Landau damping. The slow space charge wave (SSCW) becomes unstable by the cut. This wave mode and LW1 connect to new poles.

The three dispersion roots are presented in Fig. 9. There is a clear asymmetry between the two Langmuir roots, and the negative root (LW1) has solutions above $-\omega_p$. In the low k limit this is a result from the linear term in k by the centre of momentum Doppler shift in the non-stationary distribution. For shorter wavelengths this is due to the connection of the positive Langmuir root with a fast space charge wave ($\omega > \omega_p$). The positive Langmuir root (LW2) is Landau damped by the thermal spread in the beam but the imaginary part of the negative root is (in this phase velocity region) determined by the background plasma. LW1 is thus more strongly damped (solid lines) and it is also more sensitive to the suppressed high velocity tail. The unstable bandwidth in the SSCW is $\omega \in [0, 1.3]\omega_p$. Unstable solutions above ω_p are a common feature with warm plasma components ($v_t \sim v_d$) and it is not an effect of the suppressed tails.

If the expansion method is used to approximate a collection of Maxwellian distributions in temperature and density regions near those in Table III, some notes about the errors are appropriate. The growing part of the SSCW has a small E1 error, if $\Re(\omega/k)$ is in this central part of the distributions, and a non-existent E2 error in the lower half plane. For clearly unstable solutions the

TABLE III: Parameters used in the beam-plasma examples. The total plasma frequency ω_p and the beam drift v_d are used as scaling parameters. The background plasma has index $l = 1$ and the beam has $l = 2$. The difference between the two cases A1 and A2 is the introduced cut (in A2) at $v = v_t$ in the stationary distribution.

	$\omega_{p,1}^2$	$v_{t,1}$	$v_{d,1}$	m_1	n_1	$x_{0,1}$	$\omega_{p,2}^2$	$v_{t,2}$	$v_{d,2}$	m_2	n_2	$x_{0,2}$
A1	$0.9\omega_p^2$	$0.4v_d$	0	3	0	-	$0.1\omega_p^2$	$0.25v_d$	v_d	3	0	-
A2	$0.9\omega_p^2$	$0.4v_d$	0	3	3	1.0	$0.1\omega_p^2$	$0.25v_d$	v_d	3	0	-

errors are small. For marginally unstable systems it is hard to determine the points were ω/k crosses the real axis, especially if $\Re(\omega/k)$ is more than a few thermal velocities from the components drift velocities $v_{d,l}$. The other roots are strongly damped and in phase velocity regions where the parameterization method is rough.

V. MAPPING OF THE DISTRIBUTION FUNCTION IN CONSERVATIVE FIELDS

When a known velocity distribution changes under the influence of conservative forces, like e.g. electrostatic sheaths or magnetic mirror fields, it will prove useful to perform a mapping of the distribution function. By mapping the residues and poles, instead of recalculating the velocity distribution for each new position, the computational efforts can be reduced. This mapping also gives a better understanding of the introduced modifications.

Assume that the poles $\tilde{b}_i$ and residues $\tilde{a}_i$ of the distribution function $\tilde{f}(r,v) = \sum \frac{\tilde{a}_i(\phi(r))}{v-\tilde{b}_i(\phi(r))}$ are known in a point in space, say $r = 0$, where the potential energy is at minimum $\phi = 0$. The particles enters a region with a monotonic retarding potential $\phi(r)$, that approaches infinity for large r, i.e., an infinite mirror. Hence the distribution function will be symmetric around $v = 0$. The total particle energy, $\frac{mv^2}{2} + \phi$, is conserved and thus $\tilde{f}(r,v) = \tilde{f}(0, \pm\sqrt{v^2 + 2\phi(r)/m})$.
For all distribution functions that are symmetric around $v = 0$ the poles come in pairs so that for each pole $\tilde{b}_i(0)$ with residue $\tilde{a}_i(0)$ there is another pole $-\tilde{b}_i(0)$ whose residue is $-\tilde{a}_i(0)$. We here perform the calculation of the mapped poles and their residues for such a pair of poles. The part of the distribution function that is described by the considered pair is

$$f_p(0,v) = \frac{\tilde{a}_i(0)}{v-\tilde{b}_i(0)} - \frac{\tilde{a}_i(0)}{v+\tilde{b}_i(0)} = \frac{2\tilde{a}_i(0)\tilde{b}_i(0)}{v^2 - b_i^2(0)}, \quad (17)$$

where $\Im\tilde{b}_i(0) > 0$. At $r \neq 0$, where $\phi > 0$ this becomes

$$f_p(r,v) = \frac{2\tilde{a}_i(0)\tilde{b}_i(0)}{v^2 + \frac{2\phi}{m} - \tilde{b}_i^2(0)} = \frac{2\tilde{a}_i(0)\tilde{b}_i(0)}{\left(v-\tilde{b}_i(\phi)\right)\left(v+\tilde{b}_i(\phi)\right)}, \quad (18)$$

where $\tilde{b}_i(\phi) = \sqrt{\tilde{b}_i^2(0) - \frac{2\phi}{m}}$, and the square root function is chosen so that $\tilde{b}_i(\phi)$ is in the upper half plane. This can be rewritten as

$$f_p(r,v) = \frac{\tilde{a}_i(\phi)}{v-\tilde{b}_i(\phi)} - \frac{\tilde{a}_i(\phi)}{v+\tilde{b}_i(\phi)},$$

where

$$\begin{cases} \tilde{b}_i(\phi) = \sqrt{\tilde{b}_i^2(0) - \frac{2\phi}{m}},\ \Im\tilde{b}_i(\phi) > 0 \\ \tilde{a}_i(\phi) = \tilde{a}_i(0) \cdot \frac{\tilde{b}_i(0)}{\tilde{b}_i(\phi)} \end{cases}. \quad (19)$$

It is useful to write the distribution function as a sum, $\tilde{f}(0,v) = \sum_{\tilde{b}_i(0)\in U} \frac{\tilde{a}_i(0)}{v-\tilde{b}_i(0)} - \frac{\tilde{a}_i(0)}{v+\tilde{b}_i(0)}$, over the poles in the upper half plane and map $\tilde{a}_i(0)$ and $\tilde{b}_i(0)$ according to Eq. 19. When dispersion relations are calculated the lower half plane does not need to be considered at all.

In the case of a finite mirror, $\phi(r) < \infty$, particles with energies over a certain level are collected instead of reflected. This cutoff is introduced at that energy level through the use of a mask as described in section II. Since the cut T is a smooth function, and not a perfect cut, this must be seen as an approximation.

VI. SUMMARY

A flexible form for parameterization of distribution functions is presented. A low velocity expansion of Maxwellian distributions is combined with a cut in the tails represented by a Butterworth mask. With general filters and with a collection of components almost any distribution function can be described. The high velocity tail follows an inverse power law. The distribution is characterized by a vector of residues and simple poles. From the simple pole expansion it is cheap to calculate all converging moments and thus to normalize the distribution. The parameterization is used to derive linear dispersion relations. By this parameterization technique it is possible to study kinetic modifications in collisionless plasmas with non-Maxwellian distributions. It can also be used as an asymptotic Maxwellian expansion to get simple expressions that are easy to code. The expansion has small relative deviation from the Maxwellian for $v < v_t\sqrt{2}(m!)^{1/2m}$, and small absolute error for all real velocities. In a wave picture all phase velocities in this region are well described if the Landau damping is not to strong. The Landau damping does not go fast enough to zero in the long wavelength regime but the real part is well described. The smallest errors are obtained for

growing waves but again the imaginary part is uncertain close to the real phase velocity axis. Error estimates can be obtained by performing the calculations for different degrees of the expansion. More terms in the expansion gives higher converging moments, more strongly suppressed Landau damping and more Maxwell-like description in both the high and the low phase velocity region.

Acknowledgment

This work was supported by the Swedish Natural Science Research Council. We wish to thank Dr. Michael Raadu for valuable discussions.

---

* Electronic address: lofgren@plasma.kth.se

[1] R. J. Briggs, Electron-Stream Interactions with Plasmas (MIT press, Cambridge, 1964) 51
[2] D. Summers and R. M. Thorne, Phys. Fluids B **3**, 1835 (1991)
[3] L. Weinberg, Network Analysis and Synthesis (McGraw-Hill, New York, 1962) 494
[4] L. D. Landau, J. Phys (U.S.S.R.) **10**, 25 (1946)
[5] R. L. Mace and M. A. Hellberg, Phys. Plasmas **2** (6), 2098 (1995)
[6] R. M. Thorne and D. Summers, Phys. Fluids B **3**, 2117 (1991)
[7] H. Gunell, N. Brenning and S. Torvén, J. Phys. D: Appl. Phys. **29**, 643 (1996)
[8] H. Gunell, J. P. Verboncoeur N. Brenning and S. Torvén, Phys. Rev. Lett. **77**, 5059 (1996)
[9] T. M. O'Neil and J. H. Malmberg, Phys. Fluids **11**, 1754 (1968)